Phi: Jurnal Pendidikan Fisika dan Terapan
Vol.12 No.2 (2026) 49-57
ISSN: 2460-4348, e-ISSN: 2549-7162
https://jurnal.ar-raniry.ac.id/index.php/jurnalphi/index

Article Type: *orginial research*

Analysis of Electrical Properties of Activated Carbon from Empty Oil Palm Fruit Bunches (EOPFB) Against Variations in Chemical Activation Materials

Erna Krisda Wati Br Tarigan[1], Frada Erisa Pakpahan[1], Nirmala Sari[1], Rahmawati Rahmawati[1], Teuku Andi Fadlly[1*]
[1]Physics Study Program, Universitas Samudra, Langsa, Aceh, Indonesia

Correspondence E-mail: andifadly@unsam.ac.id

ARTICLE INFO

Article History:
Received: 19 January 2026
Revised: 23 March 2026
Accepted: 13 April 2026
Published: 17 April 2026

Keywords:
Activated carbon; Capacitance; Chemical activation; Conductivity

ABSTRACT

Empty Oil Palm Fruit Bunches (EOPFB) have a high organic content such as cellulose, hemicellulose, and lignin which have the potential to be used as raw materials for activated carbon. This study aims to analyze the electrical properties of activated carbon produced from EOPFB using various chemical activation materials, namely KOH, $ZnCl_2$, and $CuCl_2$. The synthesis process includes drying, carbonization at 600 °C for 1 hour and chemical activation for 24 hours. Characteristics of diffraction patterns using X-Ray Diffraction (XRD). Electrical properties of resistivity and conductivity using the 4-point probe method. In addition, the capacitance and dielectric constant using the parallel plate method. The results of this study show that the diffraction pattern of activated carbon from EOPFB generally forms an amorphous phase. Activated carbon with $ZnCl_2$ chemical activation increases the electrical conductivity, which is 1.15×10^{8} S/m compared to KOH at 4.1×10^{-1} S/m and $CuCl_2$ at 1.9×10^{-1} S/m. The capacitance value increased with chemical activation of $CuCl_2$, namely 4.44×10^{-3} F/g compared to $ZnCl_2$ at 3.8×10^{-3} F/g and KOH at 1.06×10^{-3} F/g. The dielectric constant value of activated carbon increased by using chemical activation of $CuCl_2$, namely 5.6×10^{10} compared to $ZnCl_2$ of 5.3×10^{10} and KOH of 1.5×10^{10}. It has potential as a dielectric material for capacitors.

1. PENDAHULUAN

Biomass produced from Empty Oil Palm Fruit Bunches (EOPFB) is a renewable energy source that produces environmentally friendly energy (Kongto et al., 2022). This is due to its ability to convert biomass into bioenergy such as heat, electricity, and biofuels in the form of solid, liquid and gas fuels (Terry et al., 2022). EOPFB is waste with high organic content which is often referred to as lignocellulosic waste. The main components in it are cellulose, hemicellulose, and lignin which form complex chemical bonds, making it the basic material of plant cell walls (Muryanto et al., 2023). EOPFB can be converted into activated carbon through physical or chemical activation processes. Activated carbon is a solid carbon that is commonly used as an adsorbent to adsorb liquid and gas phases (Pet et al., 2024). In addition, it is found in various allotropes such as graphite and diamond, as well as in amorphous forms

such as charcoal, carbon black, and biochar (Wang et al., 2021). Carbon can be produced from renewable and non-renewable raw materials. The precursors taken for carbon synthesis depend on the availability, price and stability of supply (Neme et al., 2022). In recent years, research has focused on developing biochar as an electrode material for energy storage devices such as batteries and supercapacitors. This material is able to store electrical energy as a dielectric material (Tamara et al., 2024).

Daily energy requirements for energy storage devices such as batteries, material cells, and supercapacitors are increasing. In general, lithium-ion batteries, often called LIBs, function as energy storage in various applications and can be used in electric vehicles (Kristiyono et al., 2022). This technology is capable of significantly reducing harmful gas emissions, making it very important to achieve carbon balance (Moon et al., 2023). Various studies have shown that variations in dielectric constant are more affected by mechanical loads or environmental conditions than electrical resistivity. This study has focused on assessing the effectiveness of various fillers of conductive materials such as steel, carbon, and graphene (Chi et al., 2023).

In previous research, activated carbon from tobacco stem core was activated using $ZnCl_2$ with a percentage ratio of activator to carbon of 2:1. These results indicate a specific capacitance of 342 F/g at a current density of 1 A/g (Ma et al., 2021). In 2025, Nahda produced activated carbon from prasman leaves using 0.2 M $ZnCl_2$ activator. In 2025, Diantoro used manihot esculenta tubers to produce activated carbon. This research was conducted using 4 M KOH activator. These results show the highest surface area and volume, namely 471.645 m^2/g and 0.253 cm^3/g (Diantoro et al., 2025). In addition, the electrochemical characteristics using symmetric coin cell supercapacitors show excellent specific capacitance of 146,570 F/g at a current of 0.1 A/g in liquid electrolyte. The electrolyte fluid uses 6 M KOH. In addition, in 2016, Yuningsih synthesized coconut shells and corn cobs into activated carbon. This is done by physical activation at a temperature of 600 ℃ for 4 hours Next, chemical activation using KOH activator with a ratio of water and carbon and KOH is 1:1:4. The results of this study show that the electrical conductivity values of activated carbon from coconut shells and corn cobs are 0.95-0.23 S/cm and 0.85-0.30 S/cm. The activated carbon produced is semiconducting, as the concentration of the activator increases the electrical conductivity value decreases (Yuningsih et al., 2016).

Based on the description that has been outlined in the previous paragraph, in this study we synthesized activated carbon from EOPFB with physical and chemical activation. Chemical activation using variations of activator materials KOH, $ZnCl_2$, and $CuCl_2$. This research is expected to have superior electrical properties, namely conductivity, capacitance, and dielectric constant. This can be applied to battery and supercapacitor technology

2. METODE

EOPFB obtained from the Prima Jasa Cooperative Palm Oil Processing Factory is cut into small pieces, then washed with distilled water until dirt or dust is removed, the next process is drying in the sun and in an oven at a temperature of 120 ℃ for 30 minutes. The EOPFB carbonization process was carried out at a temperature of 600 ℃ for 1 hour. The results were subjected to a chemical activation process using variations of three activators, namely KOH, $ZnCl_2$, and $CuCl_2$. Use of 2 M KOH, where the KOH is first dissolved in 1000 mL of distilled water. For $ZnCl_2$ and $CuCl_2$ 0.07 M, each was dissolved in 100 mL of distilled water. Next, each solution was put into a 1000 mL beaker containing 46 grams of activated carbon and soaked for 24 hours (Rahmawati et al., 2019). The next process is that each solution is filtered and washed using distilled water until the pH is 7. After the activated carbon sediment is formed, it is ground with a mortar and filtered using a 100 mesh sieve. Henceforth, each variation of activated carbon sample is named KOH Carbon, Zn Carbon, and Cu Carbon. Identification of material phases was carried out using X-Ray Diffraction (XRD).

Electrical property analysis using the 4-point probe method. This method measures the input current and output voltage values to determine the resistivity and conductivity of the material. Before carrying out the 4-point probe test, first prepare the sample. The initial stage of making a Polyvinyl Alcohol (PVA) suspension, where 15 mL of distilled water is added with 1 gram of PVA and stirred using

a magnetic stirrer for 30 minutes at a temperature of 90 °C. PVA suspension is used to form activated carbon paste. The ratio of PVA suspension to activated carbon is 1:3. The mixture is then stirred using a magnetic stirrer at 40 °C until a paste forms. The paste was deposited on ITO (Indium Tin Oxide) conductive glass with a size of 1 cm × 1 cm with a thickness of 1 mm (Rosmalinda et al., 2021). The design for measuring electric current and voltage using the 4-point probe method can be shown in Figure 1.

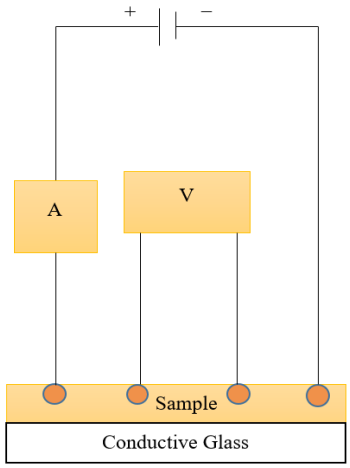

Figure 1. 4-point probe measurement design.

Electrical resistivity and electrical conductivity are calculated using equations 1 and 2 (Hajagos et al., 2025).

$$\rho = R\frac{A}{l} \tag{1}$$

$$\sigma = \frac{1}{\rho} \tag{2}$$

Where ρ is resistivity (Ωm), R is resistance (Ω), A is cross-sectional area (m^2), l is the distance between probes (m), and σ is conductivity (S/m).

Capacitor capacitance testing is conducted using the two-parallel-plate method. The setup employs two PCB boards as capacitor plates, each measuring 2 cm × 2 cm with a separation distance of of 0.5 cm. The design of the measurement setup is shown in Figure 2.

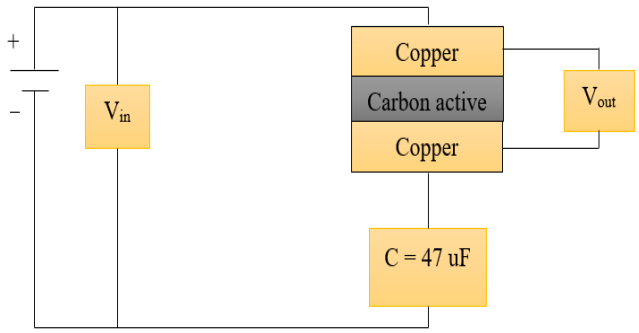

Figure 2. Design of measurement method of two parallel plates.

The capacitance and dielectric constant values can be calculated using equations 3 and 4 (Parnasari et al., 2022).

$$C_1 = \frac{C_2}{(\frac{V_{in}}{V_{out}} - 1)} \quad (3)$$

$$k = \frac{C.d}{\varepsilon_0.A} \quad (4)$$

C_1 is the capacitance of the parallel plate capacitor (F), C_2 is the capacitance of the comparison capacitor (F), d is the distance between the capacitor plates (m), k is the dielectric constant, A is the plate area (m^2), $\mathcal{E}_0$ is the permittivity of the vacuum (F/m), V_{in} is the input voltage (V), and V_{out} is the output voltage (V).

3. HASIL DAN PEMBAHASAN

Activated carbon from EOPFB produced using physical and chemical activation methods can be seen in Figure 3

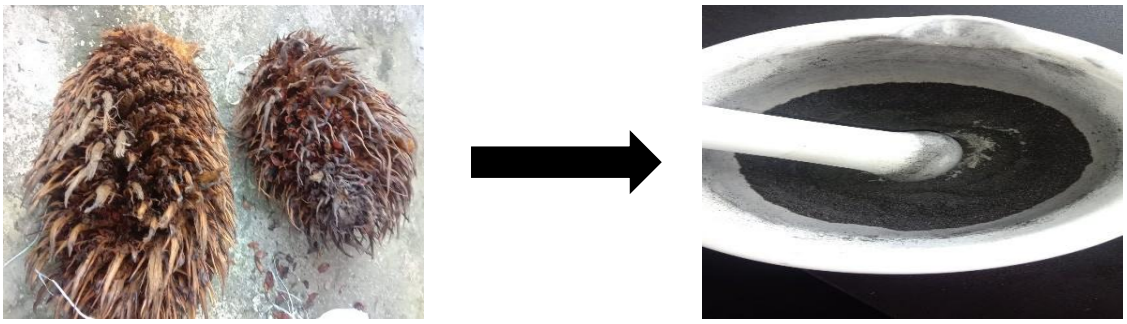

(a) (b)

Figure 3. (a) EOPFB and (b) Activated carbon from EOPFB.

Based on Figure 3, it can be seen from the physical form that the activated carbon from EOPFB has a thick black color that is odorless and in powder form. These results are also found in other organic materials (Maslahat et al., 2022).

Activated carbon that has been chemically activated with KOH, $ZnCl_2$, and $CuCl_2$ was subjected to X-Ray Diffraction (XRD) testing in powder form. The results of the XRD test can be seen in Figure 4 which provides information on the intensity peaks at an angle of 2θ.

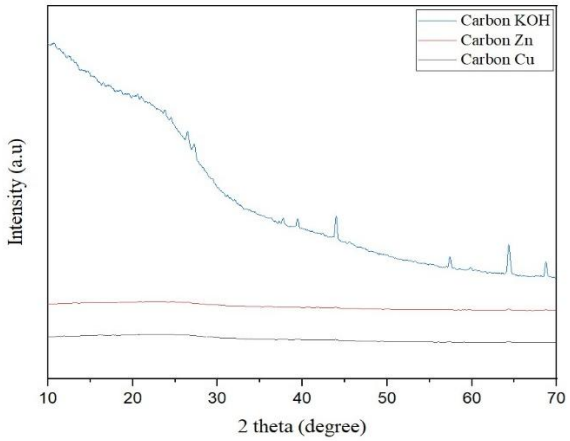

FIgure 4. Diffraction patterns of activated carbon with variations in chemical activation materials.

Based on Figure 4, the diffraction patterns of the Cu Carbon and Zn Carbon samples in the graph show amorphous characteristics with a background pattern without sharp peaks in the 2θ angle range between 10°-70°. These results correspond to COD 7132144 for Carbon Co and COD 1554684 for Carbon Zn. This shows that both samples have a low level of crystallinity or are even non-crystalline. The use of CuCl2 as an activated carbon activator was also carried out by Yao, where the diffraction pattern was observed to monitor changes in the crystal structure (Yao et al., 2023). These results show two diffraction peaks at 2θ of 24° and 43° with the (002) and (100) planes of graphitic carbon. However, the weak diffraction intensity indicates low crystallinity, thus creating a background pattern. Next, Varela used $ZnCl_2$ as an activator for biochar from corn cobs which showed a largely amorphous diffraction pattern. In addition, the crystalline phase of the Zn^{2+} compound was not found, indicating that the acid treatment removed the remaining activator and inorganic oxides (Varela et al., 2024).

In contrast, the diffraction pattern of KOH activated carbon shows several clear sharp peaks, especially at 2θ angles of 43.96° and 64.32°. The peaks identify CsInMnSe corresponding to COD 7151240, but in general the diffraction pattern is background or amorphous. The same thing was reported by Hardi that the crystallite structure of EOPFB activated carbon showed an amorphous structure with two broad peaks at 2θ angles of 26.20° and 43.08° with the (002) and (100) planes. The presence of these two broad peaks is in accordance with the data from the Joint Committee on Powder Diffraction Standards (JCPDS) No. 75-1621 which is a characteristic of activated carbon (Hardi et al., 2020).

The results of resistivity and conductivity measurements using the 4-point probe method can be seen in Table 1.

Tabel 1. Average values of resistivity and conductivity of activated carbon.

Sample	Voltage(V)	Current (A)	Resistivity (Ωm)	Conductivity (S/m)
KOH Carbon	$1{,}40\times 10^{-1}$	$0{,}01 \times 10^{-5}$	$6{,}94 \times 10^{1}$	$4{,}10 \times 10^{-1}$
Zn Carbon	$8{,}20 \times 10^{-2}$	$1{,}43 \times 10^{-5}$	$8{,}68 \times 10^{-9}$	$1{,}15 \times 10^{8}$
Cu Carbon	$1{,}50 \times 10^{-1}$	$1{,}37 \times 10^{-5}$	$5{,}40 \times 10^{0}$	$1{,}90 \times 10^{-1}$

Based on Table 1, it can be seen that the current has a great influence on the value of voltage, resistivity and conductivity. In the KOH Carbon sample, the resistivity value is 6.94 × 101 Ωm and the conductivity value is 4.1×10^{-1} S/m. Previous research has reported that rice husk-based activated carbon can be effectively synthesized via chemical activation using KOH, which enhances porosity and electrochemical performance due to the development of well-defined pore structures (Barakat et al., 2023). Based on conductivity measurements using the four-point probe method, the electrical conductivity of rice husk activated carbon typically falls within a range influenced by microstructure and particle connectivity (Nandi et al., 2023).

The Carbon Zn sample has the lowest resistivity value, namely 8.68×10^{-9} Ωm and the highest conductivity value of 1.15×10^{8} S/m, this shows that Carbon Zn is the best electrical conductor of the other samples. This behavior is consistent with previous studies showing that materials with well-developed conductive networks, particularly carbon- or graphene-based systems, exhibit very high electrical conductivity and correspondingly low resistivity due to efficient charge transport mechanisms (Tarhini & Tehrani-Bagha, 2023).

The Cu Carbon sample has the highest resistivity value, namely 5.40×10^{0} Ωm and the lowest conductivity value, namely 1.9×10^{-1} S/m. This shows that the conductivity value of graphene is greater than that of the Carbon Zn sample. Poor conductive pathways in a material lead to low electrical conductivity and correspondingly high resistivity (Zare et al., 2024). This behavior is consistent with

previous studies showing that materials with weak or poorly connected conductive networks exhibit high resistivity and low electrical conductivity due to inefficient charge transport (Liu et al., 2022). The capacitance of activated carbon with variations in chemical activation materials is presented in Figure 5. This figure shows a graph between capacitance and voltage.

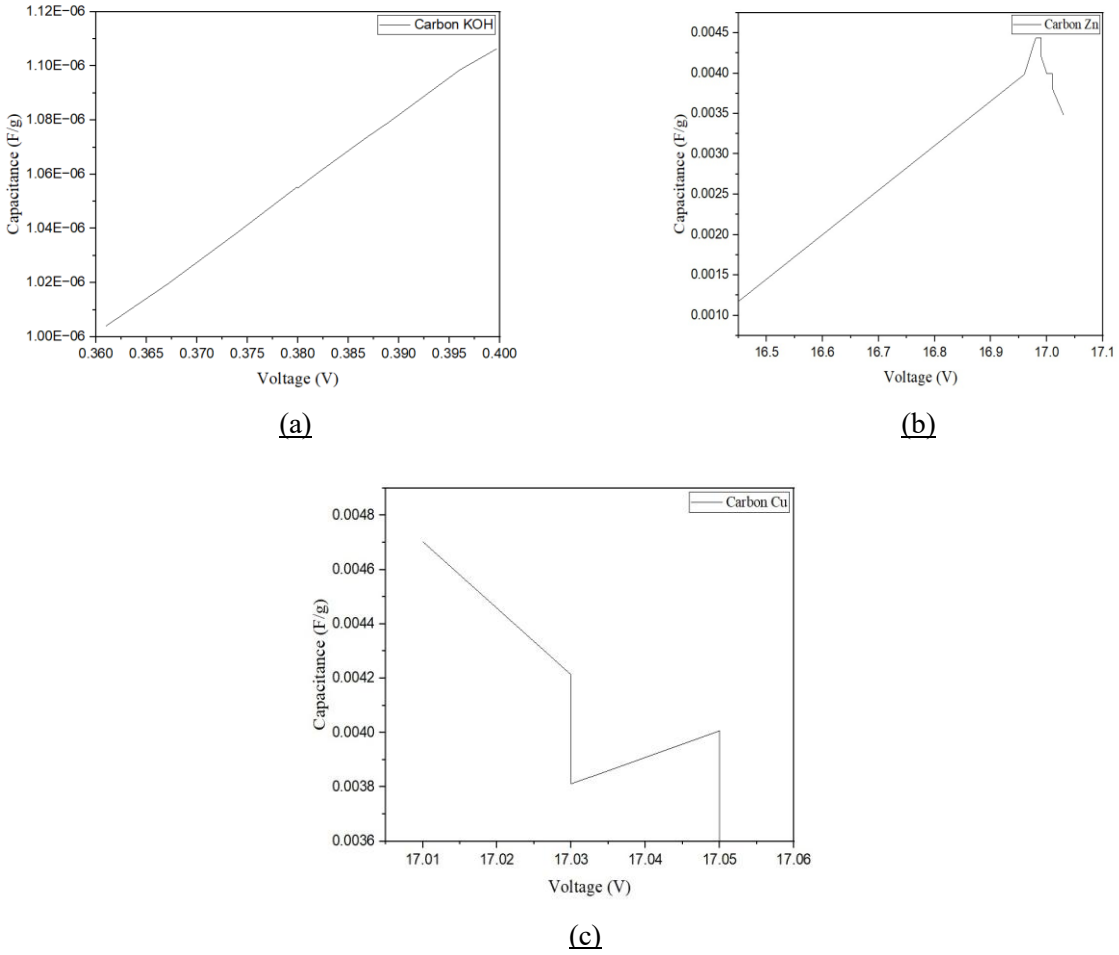

Figure 5. Capacitance graph against electric voltage, (a) KOH carbon, (b) Zn carbon, and (c) Cu carbon.

Based on Figure 5.a, it can be seen that the capacitance of KOH Carbon shows a positive linear increase along with the increase in voltage. The highest capacitance value of Carbon KOH is 0.01 × 10^{-3} F/g. The research used KOH as an activator on activated carbon from rice husk with a concentration of 30%, the test results on supercapacitor cells with Cu Foil substrate and 2 M KOH electrolyte obtained a specific capacitance value of 8.56 F/g using a scan rate of 25 mV/s (Huda et al., 2022).

Based on Figure 5.b, the highest capacitance value for Carbon Zn is 4.44 × 10^{-3} F/g. In Ma's research on activated carbon from tobacco stems activated using ZnCl2 precursor with a ratio of 2:1, it showed a capacitance of 342 F/g. This shows that tobacco stem core carbon is promising as an electrode material (Ma et al., 2021). The comparison of the capacitance value of Carbon Zn is still far from the results of Ma's research. Furthermore, Figure 5.c Cu carbon shows a unique and different pattern compared to KOH or Zn carbon. At the beginning of the range between 17.01 V to 17.03 V, the capacitance drops from 5.3 × 10^{-3} F/g to 4.7 × 10^{-3} F/g. Subsequently, there is a sharp decrease to 3.3 × 10^{-3} F/g at a voltage of 17.05 V. The capacitance value of activated carbon determines the dielectric constant. The average dielectric constant values for various chemical activation materials are shown in Table 2.

Table 2. Average value of dielectric constant of activated carbon.

Sample	V_{in} (V)	V_{out} (V)	Capacitance (F/g)	Dielectric Constant
KOH Carbon	17,31	0,38	$0{,}01 \times 10^{-3}$	$1{,}5 \times 10^{10}$
Zn Carbon	17,19	16,94	$3{,}80 \times 10^{-3}$	$5{,}3 \times 10^{10}$
Cu Carbon	17,25	17,04	$4{,}44 \times 10^{-3}$	$5{,}6 \times 10^{10}$

Based on Table 2, it shows that Zn Carbon and Cu Carbon have much higher capacitance and dielectric constant values than KOH Carbon. Carbon Zn and Cu can be used as dielectric materials in capacitors because they have high dielectric constants and capacitance, so they can store more energy. Chemically activated carbon with KOH can be used for applications requiring high electrical conductivity, such as electrodes in capacitors (Ghosh et al., 2025). In previous studies, it was stated that KOH carbon is superior for electrodes, while metal-modified carbon is more suitable as a dielectric material (Cheng et al., 2019). Further research on the CNTs system doped with ZnO@CuO improves the dielectric quality and capacitance (Sanni et al., 2025). This material can be used as a supporting electrode material for capacitors.

4. CONCLUSION

Biomass from EOPFB can be used as a base material for activated carbon. The diffraction patterns of Zn Carbon and Cu Carbon show an amorphous phase with a background pattern. Furthermore, KOH carbon shows sharp peaks at 2θ angles of 43.96° and 64.32° which indicates the presence of a crystalline structure compared to the two previous activators, although the dominant one remains amorphous. The highest conductivity of activated carbon is in the Zn Carbon sample, namely 1.15 × 108 S/m compared to Cu and Zn carbon. Furthermore, the highest dielectric constant value of activated carbon is found in the Cu Carbon sample, namely 5.6 × 1010 compared to Zn carbon and KOH.

REFERENCES

Barakat, N. A. M., Irfan, O. M., & Moustafa, H. M. (2023). H3PO4/KOH Activation Agent for High Performance Rice Husk Activated Carbon Electrode in Acidic Media Supercapacitors. *Molecules*, *28*(1), 296. https://doi.org/10.3390/molecules28010296

Cheng, Y., Hao, Z., Hao, C., Deng, Y., Li, X., Li, K., & Zhao, Y. (2019). A review of modification of carbon electrode material in capacitive deionization. *RSC Advances*, *9*(42), 24401–24419. https://doi.org/10.1039/c9ra04426d

Chi, V. M., Hai, N. M., Lan, N., & Huong, N. V. (2023). An empirical model for electrical resistivity of mortar considering the synergistic effects of carbon fillers, current intensity, and environmental factors. *Case Studies in Construction Materials*, *19*(1), e02685. https://doi.org/10.1016/j.cscm.2023.e02685

Diantoro, M., Aturroifah, N. I. M., Utomo, J., Luthfiyah, I., Hamidah, I., Yuliarto, B., Rusydi, A., Meevesana, W., Maensiri, S., & Singh, P. K. (2025). Optimizing sponge-like activated carbon from Manihot esculenta tubers for high-performance supercapacitors. *Arabian Journal of Chemistry*, *18*(1), 106068. https://doi.org/10.1016/j.arabjc.2024.106068

Ghosh, S., Zhang, Y., Pagani, G., Suriano, R., Agozzino, M., Jastrzębska, A., & S. Casari, C. (2025). KOH-activated micrometer-thick amorphous carbon nanofoam as a binder-free supercapacitor electrode with high-rate performance. *Chemical Communications*, *61*(68), 12797–12800. https://doi.org/10.1039/D5CC01916H

Hajagos, S., Kovács, J. G., Suplicz, A., Széplaki, P., & Zink, B. (2025). An experimental and theoretical study on the electrical conductivity of polymer composites. *Journal of Materials Research and Technology*, *39*(1), 6300–6309. https://doi.org/10.1016/j.jmrt.2025.10.217

Hardi, A. D., Joni, R., Syukri, S., & Aziz, H. (2020). Pembuatan Karbon Aktif dari Tandan Kosong Kelapa Sawit sebagai Elektroda Superkapasitor. *Jurnal Fisika Unand*, *9*(4), 479–486. https://doi.org/10.25077/jfu.9.4.479-486.2020

Huda, A. N., Lestari, I., & Hidayat, S. (2022). Pemanfaatan Karbon Aktif dari Sekam Padi Sebagai Elektroda Superkapasitor. *JIIF (Jurnal Ilmu dan Inovasi Fisika)*, *6*(2), 102–113. https://doi.org/10.24198/jiif.v6i2.39639

Kongto, P., Palamanit, A., Ninduangdee, P., Singh, Y., Chanakaewsomboon, I., Hayat, A., & Wae-hayee, M. (2022). Intensive exploration of the fuel characteristics of biomass and biochar from oil palm trunk and oil palm fronds for supporting increasing demand of solid biofuels in Thailand. *Energy Reports*, *8*(1), 5640–5652. https://doi.org/10.1016/j.egyr.2022.04.033

Kristiyono, R., Nugroho, B., & Supriyanto, B. (2022). Automatic charging battery lithium untuk kendaraan listrik. *Teknika*, *7*(4), 236–242. https://doi.org/10.52561/teknika.v7i4.195

Liu, H., Deshmukh, A., Salowitz, N., Zhao, J., & Sobolev, K. (2022). Resistivity Signature of Graphene-Based Fiber-Reinforced Composite Subjected to Mechanical Loading. *Frontiers in Materials*, *9*(1), 1–11. https://doi.org/10.3389/fmats.2022.818176

Ma, Z., Jiang, B., Yuan, Q., Cao, L., Liu, L., Tian, J., Huang, Z., Zong, Z., Lin, Z., Zhang, P., & Wang, J. (2021). Tobacco stalks core-derived activated carbon with high capacitance by ZnCl2 for supercapacitors. *Vibroengineering PROCEDIA*, *39*(1), 114–119. https://doi.org/10.21595/vp.2021.22275

Maslahat, M., Kamalia, E., & Arrisujaya, D. (2022). Sintesis dan karakterisasi mikro partikel karbon aktif tandan kosong kelapa sawit. *Analit : Analytical and Environmental Chemistry*, *7*(2), 177–188. https://doi.org/10.23960/aec.v7i02.2022.p177-188

Moon, J., Yun, H., Ukai, J., Chokradjaroen, C., Thiangtham, S., Hashimoto, T., Kim, K., Sawada, Y., & Saito, N. (2023). Correlation function of specific capacity and electrical conductivity on carbon materials by multivariate analysis. *Carbon*, *215*(1), 118479. https://doi.org/10.1016/j.carbon.2023.118479

Muryanto, M., Sudiyani, Y., Darmawan, M. A., Handayani, E. M., & Gozan, M. (2023). Simultaneous Delignification and Furfural Production of Palm Oil Empty Fruit Bunch by Novel Ternary Deep Eutectic Solvent. *Arabian Journal for Science and Engineering*, *48*(12), 16359–16371. https://doi.org/10.1007/s13369-023-08211-y

Nandi, R., Jha, M. K., Guchhait, S. K., Sutradhar, D., & Yadav, S. (2023). Impact of KOH Activation on Rice Husk Derived Porous Activated Carbon for Carbon Capture at Flue Gas alike Temperatures with High CO2/N2 Selectivity. *ACS Omega*, *8*(5), 4802–4812. https://doi.org/10.1021/acsomega.2c06955

Neme, I., Gonfa, G., & Masi, C. (2022). Activated carbon from biomass precursors using phosphoric acid: A review. *Heliyon*, *8*(12), e11940. https://doi.org/10.1016/j.heliyon.2022.e11940

Parnasari, P., Nurhanisa, M., & Nugroho, B. S. (2022). Studi Kapasitansi dan Konstanta Dielektrik Pada Karbon Aktif Tandan Kosong Kelapa Sawit. *PRISMA FISIKA*, *10*(1), 98–104. https://doi.org/10.26418/pf.v10i1.54333

Pet, I., Sanad, M. N., Farouz, M., ElFaham, M. M., El-Hussein, A., El-sadek, M. S. A., Althobiti, R. A., & Ioanid, A. (2024). Review: Recent Developments in the Implementation of Activated Carbon as Heavy Metal Removal Management. *Water Conservation Science and Engineering*, *9*(2), 62. https://doi.org/10.1007/s41101-024-00287-3

Rahmawati, R., Fadlly, T., & Harmawan, T. (2019). Karakterisitik energi gap (Eg) komposit ZnO/karbon aktif dari tandan kosong kelapa sawit (Elaeis guineensis Jack) untuk aplikasi sel surya. *Jurnal Fisika*, *9*(2), 60–68. https://doi.org/10.15294/jf.v9i2.23334

Rosmalinda, R., Rahmawati, R., & Fadlly, T. A. (2021). Pengaruh Variasi Karbon Aktif dari TKKS Pada TiO2 Terhadap Efisiensi Sel Surya DSSC Menggunakan Dye Kulit Jengkol (Pitchellobium Lobatum Benth). *Wahana Fisika*, *6*(2), 142–150. https://doi.org/10.17509/wafi.v6i2.39222

Sanni, A., Govindarajan, D., Nijpanich, S., Limphirat, W., Theerthagiri, J., Choi, M. Y., & Kheawhom, S. (2025). Al-doped ZnO@CuO nanoflower/nanorod heterostructures on CNTs as high-performance supercapacitor electrodes in redox-supporting electrolytes. *Journal of Energy Storage*, *109*(1), 115184. https://doi.org/10.1016/j.est.2024.115184

Tamara, G. J., Polii, J., Tumimomor, F. R., Rampengan, A. M., & Mongan, S. W. (2024). Karakteristik I-V elektroda superkapasitor berbasis karbon aktif kulit kacang batik kawangkoan. *SOSCIED*, *7*(2), 413–420. https://doi.org/10.32531/jsoscied.v7i2.834

Tarhini, A., & Tehrani-Bagha, A. R. (2023). Advances in Preparation Methods and Conductivity Properties of Graphene-based Polymer Composites. *Applied Composite Materials*, *30*(6), 1737–1762. https://doi.org/10.1007/s10443-023-10145-5

Terry, L. M., Loy, A. C. M., Chew, J. J., How, B. S., Andiappan, V., & Sunarso, J. (2022). Chemical engineering and the sustainable oil palm biomass industry—Recent advances and perspectives for the future. *Chemical Engineering Research and Design*, *188*(1), 729–735. https://doi.org/10.1016/j.cherd.2022.10.017

Varela, C. F., Moreno-Aldana, L. C., & Agámez-Pertuz, Y. Y. (2024). Adsorption of pharmaceutical pollutants on ZnCl2-activated biochar from corn cob: Efficiency, selectivity and mechanism. *Journal of Bioresources and Bioproducts*, *9*(1), 58–73. https://doi.org/10.1016/j.jobab.2023.10.003

Wang, Y., Zeng, Q., Du, X., Gao, Y., & Yin, B. (2021). The structural, mechanical and electronic properties of novel superhard carbon allotropes: *Ab initio* study. *Materials Today Communications*, *29*(1), 102980. https://doi.org/10.1016/j.mtcomm.2021.102980

Yao, S., Li, Z., Liu, Z., Geng, X., Dai, L., & Wang, Y. (2023). CuCl2-Activated Sustainable Microporous Carbons with Tailorable Multiscale Pores for Effective CO2 Capture. *ACS Omega*, *8*(44), 41641–41648. https://doi.org/10.1021/acsomega.3c05842

Yuningsih, L. M., Mulyadi, D., & Kurnia, A. J. (2016). Pengaruh Aktivasi Arang Aktif dari Tongkol Jagung dan Tempurung Kelapa Terhadap Luas Permukaan dan Daya Jerap Iodin. *Jurnal Kimia Valensi*, *2*(1), 30–34. https://doi.org/10.15408/jkv.v2i1.3091

Zare, Y., Munir, M. T., & Rhee, K. Y. (2024). Assessment of electrical conductivity of polymer nanocomposites containing a deficient interphase around graphene nanosheet. *Scientific Reports*, *14*(1), 8737. https://doi.org/10.1038/s41598-024-59678-0